ELSEVIER

Applied Catalysis B: Environmental 18 (1998) 307–315

APPLIED CATALYSIS B: ENVIRONMENTAL

Characterization and activity of copper and nickel catalysts for the oxidation of phenol aqueous solutions

A. Alejandre[a], F. Medina[a], P. Salagre[b], A. Fabregat[a], J.E. Sueiras[a,*]

[a] *Departament d'Enginyeria Química, ETSEQ. Universitat Rovira i Virgili, Pl. Imperial Tarraco 1, 43005 Tarragona, Spain*
[b] *Facultat de Química, Universitat Rovira i Virgili. Pl. Imperial Tarraco 1, 43005 Tarragona, Spain*

Received 1 February 1998; received in revised form 7 May 1998; accepted 17 May 1998

Abstract

Catalysts based on CuO/γ-alumina, $CuAl_2O_4$/γ-alumina, NiO/γ-alumina, $NiAl_2O_4$/γ-alumina and bulk $CuAl_2O_4$ have been structurally characterized by BET, porosimetry, X-ray diffraction (XRD) and scanning electron microscopy (SEM). Their catalytic behaviors have also been tested for the oxidation of 5 g/l phenol aqueous solutions using a triphasic tubular reactor working in a trickle-bed regime and air with an oxygen partial pressure of 0.9 MPa at a temperature of 413 K. The copper and nickel catalysts supported on γ-alumina have surface areas of the same order as the support γ-alumina of ca. 190 m^2/g and high active phase dispersions which were also confirmed by SEM, whereas the bulk copper aluminate spinel has a surface area of ca. 30 m^2/g. XRD detects the phases present and shows a continuous loss of CuO by elution and the formation of a copper oxalate phase on the surface of the copper catalysts which also elutes with time. The NiO was also eluted but less than the copper catalysts. Only the copper and nickel spinel catalysts were stable throughout the reaction. Phenol conversion vs. time shows a continuous overall decrease in activity for the CuO/γ-alumina and NiO/γ-alumina catalysts. In turn, the copper and nickel spinel catalysts reach steady activity plateaus of 40 and 10%, respectively, of phenol conversion. The bulk copper aluminate spinel shows an activity plateau of 20% of the conversion which is lower than that from the copper aluminate/γ-alumina catalyst due to its lower surface area. Nickel catalysts always have lower activities than the copper catalysts for the phenol oxidation reaction. The copper catalysts drive a mechanism of partial phenol oxidation to carboxylic acids and quinone-related products with very high specific rates, and the nickel catalysts mainly drive a mechanism of CO_2 formation with lower conversion but with a potential higher catalyst life. The triphasic tubular reactor using trickle-bed regime largely avoids the mechanism of polymer formation as a catalyst deactivation process.

Keywords: Phenol oxidation; Copper catalysts; Nickel catalysts; Trickel-bed reactor

1. Introduction

In many cases, the aqueous streams caused by chemical and related industries contain organic pollutants such as phenol, which is toxic and poorly biodegradable. These polluting agents are also in very high concentrations so that direct biological treatment is not appropriate, or in very low concentrations when the recovery is not economically feasible [1]. In these cases, it is necessary to use less conventional techniques to remove the pollutants.

*Corresponding author. Tel.: +34 977 559787; fax: +34 977 559597.

0926-3373/98/$ – see front matter
PII: S0926-3373(98)00050-2

Different methods for treating industrial waste water containing organic pollutants have been widely reported. The choice of treatment depends on the level of phenol concentration, on economics and easy control, reliability and treatment efficiency [2,3,9,14].

Several processes have been studied, such as chemical oxidation [2,4–8], electrochemical treatment [9–13], wet oxidation [14–18], photo-catalytic oxidation [19], photo-electrochemical oxidation [20], processes in supercritical conditions [21–28], or burning. In many cases, several reaction conditions are required, higher temperatures (500–700 K) and pressures 70–200 bar, for oxidation to take place. In other cases, higher amounts of energy or chemical products are required. Hence, these expensive methods have lower feasibility.

The development of inexpensive and efficient processes for waste-water treatment at intermediate levels of phenol concentration is of considerable interest for industrial activities.

The oxidation of dilute aqueous solutions for organic pollutants using air or oxygen over a solid catalyst has been shown to be a useful and inexpensive alternative process in which the organic compounds are oxidised to carbon dioxide and water [29–37]. Batch and semi-batch approaches have previously been studied [29–33]. It has been recently reported [34–38] that continuous processes in a three-phase reactor in a trickle-bed regime are suitable in much milder conditions for the catalytic treatment of aqueous solutions with pollutant loading.

The catalysts which have been used until now undergo serious activity losses and deactivations due to the strong oxidation conditions of the processes used. This effect needs further investigation, and is one of the targets of this work. Here, we make a comparative study of a copper oxide/γ-alumina catalyst and four novel catalysts based on copper aluminate, nickel aluminate and nickel oxide/γ-alumina which, to our knowledge, have not yet been reported for the reaction concerned.

These solids have been prepared and structurally characterised to oxidise phenol aqueous solutions using a trickle-bed reactor.

2. Experimental

2.1. Sample preparation

Copper oxide/γ-alumina and nickel oxide/γ-alumina precursors were prepared by impregnating γ-alumina (BET area 197 m^2/g) with the corresponding copper nitrate hydrate or nickel nitrate hexahydrate aqueous solutions using the dry soaking method. The alumina support was previously ground and sieved in the 25–50 mesh range before impregnation. The samples were dried at 393 K for 5 h and then calcined at different temperatures for 8 h in air, for the catalysts labelled C-1, C-2, C-3 and C-4. Catalyst C-5 was prepared from the stoichiometric mixture of hydrated copper nitrate and aluminium nitrate nonahydrate. Calcination temperatures and the loadings obtained after calcination are listed in Table 1. All reagents were reagent-grade (from Aldrich).

2.2. BET areas

BET surface areas were calculated from the nitrogen adsorption isotherms at 77 K by using a Micromeritics ASAP 2000 surface analyser and a value of 0.164 nm^2 for the cross section of the nitrogen molecule.

Table 1
Surface characteristics of catalysts C-1, C-2, C-3, C-4 and C-5

Sample	Composition	Calcination temperature (K)	BET area (m^2/g)	Average pore diameter (nm)	Pore volume (cm^3/g)
C-1	10% CuO/γ-Al_2O_3	773	190	11.2	0.53
C-2	10% NiO /γ-Al_2O_3	773	188	11.2	0.52
C-3	10% CuO /γ-Al_2O_3	1173	187	11.3	0.52
C-4	10% NiO /γ-Al_2O_3	1173	189	11.3	0.53
C-5	$CuAl_2O_4$	1173	30	13.8	0.06

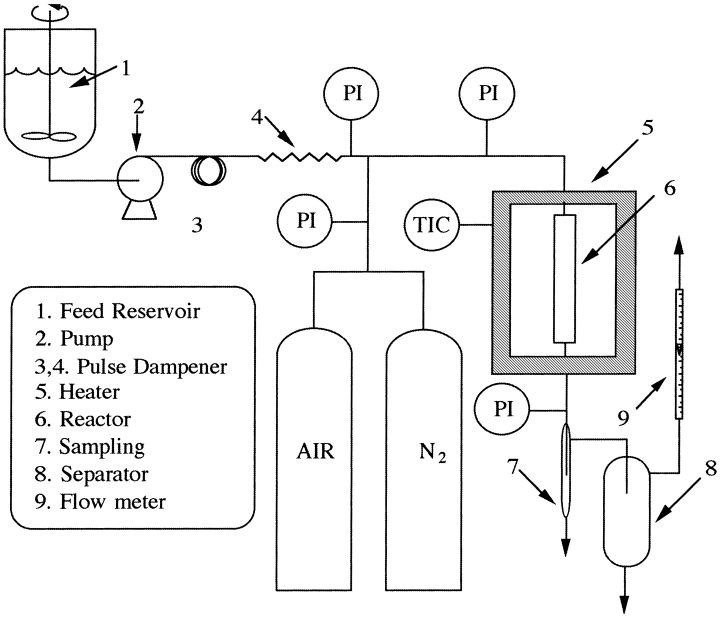

Fig. 1. Experimental setup for catalytic oxidation studies.

2.3. X-ray diffraction (XRD)

Powder X-ray diffraction (XRD) patterns of the catalysts were obtained with a Siemens D5000 diffractometer by using nickel-filtered CuK_α radiation. Samples were dusted on double-sided sticky tape and mounted on glass microscope slides. The patterns were recorded over the $5>2\Theta>85^\circ$ range and compared to the X-ray powder files to confirm phase identities. The patterns of the detected phases are: aluminium oxide (γ-alumina) (d=1.40 Å (100), 1.97 Å (80), 2.4 Å (60), 4.6 Å (40) and 2.27 Å (30)); copper oxide (tenorite) (d=2.524 Å (100), 2.311 Å (100), 2.531 Å (60) and 1.8667 Å (25)); copper oxalate hydrate (moolooite) (d=3.88 Å (100), 2.476 Å (20), 1.756 Å (18) and 1.774 Å (16)); aluminium oxide hydroxide (boehmite) (d=6.11 Å (100), 3.164 Å (65), 2.346 Å (55), 1.896 Å (30) and 1.860 Å (25)); copper aluminium oxide (d=2.436 Å (100), 2.856 Å (55), 1.4279 Å (35), 1.5542 Å (25) and 2.019 Å (16)); Nickel oxide (d=2.088 Å (100), 2.412 Å (60), 1.477 Å (35), 1.476 Å (35) and 1.260 Å (18)) and nickel aluminium oxide (d=2.427 Å (100), 2.013 Å (65), 1.4232 Å (60), 1.5485 Å (30), 4.65 Å (20) and 2.846 Å (20)).

2.4. Scanning electron microscopy (SEM)

Scanning electron micrographs were obtained with a JEOL JSM-6400 microscope operating at acceleration voltages=30 kV, working distances=8–19 mm and magnification values of 30 000×.

2.5. Determination of catalytic activity

The experimental set-up (see Fig. 1) consists of a stirred, 1-l tank connected to a high-pressure metering pump that works in a flow-rate range of 10–150 ml/h. This pump feeds a triphasic tubular reactor (1.1 cm i. d. and 20.0 cm long), operating in a trickle-bed regime and heated by an oven equipped with a temperature control system. The reactor was filled with the catalysts, previously ground and sieved in the 25–50 mesh range.

The air was directly fed in from a high-pressure gas cylinder after reaching the desired value. The products of the reaction were rapidly cooled, before separating the liquid and gas phases, into two vessels, the smallest of which was used for liquid sampling. The gases were measured with a flow-meter that also worked as a gas-flow controller. Both, the feed and the different

reaction products were analysed by high-performance liquid chromatography (Beckman System Gold, HPLC) to determine the phenol conversion and product distribution, using Spherisorb ODS2 ($25\times0.4\ cm^2$) as a stationary phase and a mixture of 35% methanol (HPLC quality) and 65% bidistilled water at pH 2.5 with H_2SO_4 as a mobile phase. Flow rate of the mobile phase was set to be 1 ml/min. A UV spectrophotometer at λ=254 nm was employed as detector. For the analysis of carboxylic acids and quinones, a method with changing the methanol/water ratio in the mobile phase and two different λ values, such as 219 and 254 nm, was used. The weight percentage of total carbon difference between the feed and the sum of the reaction organic products, determined by HPLC, was assumed to be the CO_2 released by the reaction [34,37]. To evaluate the error of this assumption, the expected COD (chemical oxygen demand from total organic matter) values from the HPLC results (feed and total reaction organic products) were compared with the experimental COD values determined by the standard method of $Cr_2O_7^{2-}/Cr^{3+}$ reduction and UV-visible spectroscopy determination of Cr^{3+}. The results of both methods gave deviations which were always lower than 2%. The fairly good agreement between both techniques accounted for the HPLC sound analysis of the whole product range obtained, and allowed us to determine the conversion of phenol to carbon dioxide. The amount of carbon dioxide was also obtained (for one test), by the determination of barium carbonate obtained when the gas outlet stream was continuously bubbled into a saturated barium hydroxide solution [32]. The deviations with this method were always lower than 4%.

This work shows the results of the catalytic removal of phenol in the aqueous phase, and, in particular, the results of the catalytic oxidation of an aqueous solution of 5 g/l in phenol using air as oxidant. The reaction conditions were as follows: the reaction temperature was 413 K, the gas flow rate 2.3 ml/s, the liquid flow rate 35.4 ml/h working at 0.41 h of inverse WHSV (weight hourly space velocity), the partial oxygen pressure was maintained at 0.9 MPa, the particle diameter of the catalysts was 25–50 mesh, and 14.52 g of the catalyst was loaded into the reactor. The standard tests of diffusional limitations through the catalysts revealed the absence of limitations by external and internal mass transfers. For this purpose, several experiments were performed, changing the weight catalyst between 5 and 20 g and the particle diameter in the 25–110 mesh range, maintaining the residence time (0.41 h) [39]. The conversion values were always similar to those of Fig. 3 (zone of plateaus of conversions).

3. Results and discussion

3.1. Bet areas

Table 1 collects the results obtained from the BET and porosimetry determinations which include the BET surface area, the average pore diameter (nm) and the pore volume of the catalysts. Small differences have been observed in the C-1 to C-4 BET surface areas and pore volumes, and with respect to the support (γ-alumina of 197 m^2/g). The BET surface area is ca. 190 m^2/g and the average pore diameter 11 nm. Supported catalysts C-1 to C-4 basically retain the surface properties of the support. We can assume that the CuO and the NiO phases are well dispersed on the support and do not gives rise to any significant change in porosities, even at higher calcination temperature such as 1173 K. This high dispersion of the catalysts active phases has also been detected using other techniques such as XRD and SEM. The low surface area (30 m^2/g) and pore volume of the C-5 sample are indicative of the fact that its pore density is lower than catalysts C-1 to C-4. This is because of the strong agglomeration of the material produced by the higher calcination temperature and by the formation of a new pure phase such as copper aluminate.

3.2. X-ray diffraction (XRD)

Table 2 summarises the crystalline phases detected by XRD before, during (analysing at different reaction times) and after the reaction process for the catalysts being studied. Before reaction, the crystal phases detected are related with the calcination temperature of the sample. At lower calcination temperatures (773 K), the detected phases shown in Table 2 are γ-alumina together with CuO and NiO for catalysts C-1 and C-2, respectively. However, at higher calcination temperatures (1173 K), the detected phases are

Table 2
XRD characterization of catalysts C-1 to C-5 [a]

Sample	XRD phase detected		
	before reaction	during reaction	after reaction
C-1	γ+T	γ+M+B+T	B
C-2	γ+N	γ+B+N	B
C-3	γ+S1	γ+M+B+T+S1	B+S1
C-4	γ+S2	γ+B+N+S2	B+S2
C-5	S1	S1	S1

[a] Here, γ stands for γ-alumina (γ-Al_2O_3); M for moolooite (CuC_2O_4 $n{\cdot}H_2O$); S1 for spinel-phase ($CuAl_2O_4$); S2 for spinel-phase ($NiAl_2O_4$); B for boehmite (ALOOH); T for tenorite (CuO); and N for bunsenite (NiO).

γ-alumina for C-3 and C-4 catalysts, and spinel phases $CuAl_2O_4$ for C-3, and C-5, and $NiAl_2O_4$ for C-4 catalysts, produced by interactions between the copper or nickel oxide and the alumina [37,40,44,45].

The crystal phases of the catalysts C-1 to C-4 change quite considerably before, during and after the reaction. Catalyst C-1 shows γ-alumina and tenorite (CuO) phases before the reaction, γ-alumina, moolooite (CuC_2O_4), boehmite (AlOOH) and tenorite during the reaction and only boehmite after the reaction (1000 h). Thus, under the reaction conditions tested, the CuO phase disappears with time. Catalyst C-2 shows γ-alumina and bunsenite (NiO) before reaction, γ-alumina, boehmite and bunsenite during reaction and only boehmite after the reaction. Thus, under the reaction conditions tested, the NiO phase also disappears with time.

Table 2 also shows that the spinel structure of catalysts C-3 and C-4 ($CuAl_2O_4$ and $NiAl_2O_4$ respectively) remains stable as a function of time but the phase of the support changes from γ-alumina to boehmite. Traces of moolooite+tenorite and bunsenite were also detected for catalysts C-3 and C-4, respectively, during the reaction. These phases came from the copper and nickel oxides which did not react with the aluminium oxide during the calcination process at higher temperatures to form the corresponding aluminate. The reaction conditions, (aqueous phase and both, higher temperature (>413 K) and pressure (>40 atm)), may improve the crystallinity of the copper and nickel oxide particles [37]. Therefore, these crystalline phases (tenorite and bunsenite) can be detected in some catalysts during the reaction process, although they were not detected for the fresh catalysts.

Catalyst C-5, made up of pure copper aluminate, remains stable during the reaction conditions tested.

From Table 2, it can also be observed that the reaction process containing catalysts C-1 and C-3 causes the formation of a new crystalline phase such as copper oxalate, moolooite (CuC_2O_4 nH_2O), the latter showing a good crystallinity. This copper oxalate phase may be formed either by the reaction of the oxalic acid, obtained during the reaction pathway shown in Fig. 5 [32,37], with the copper oxide on the surface of the catalyst, or by the precipitation of copper oxalate assuming that copper ions are obtained from copper oxide elution with the organic acids, yielded during the process, It should be pointed out that we did not detect nickel oxalate on the surface of catalysts C-2 and C-4 during the reaction process.

During the reaction process, it was also observed that the support (γ-alumina) evolves into a new phase detected as boehmite (AlOOH) in catalysts C-1 to C-4. This new crystalline phase may be formed because of the reaction conditions, that is to say, the aqueous phase and both, higher temperature (>413 K) and pressure (>40 kg/cm^2). Hence, according to the XRD results, catalysts C-1 to C-4 become unstable under the reaction conditions used, whereas catalyst C-5 does not.

3.3. Scanning electron microscopy (SEM)

The electron microscopy technique shows that the copper and nickel oxides of the fresh catalysts C-1 and C-2, respectively, are highly dispersed. No large CuO or NiO particles (particles sizes smaller than 10 nm) were detected on the γ-alumina surface under magnification of 30 000×, as shown in Fig. 2, in agreement with the XRD and X-ray analysis. As a result, mappings of the copper and nickel oxides on the catalyst using X-ray analysis at lower voltages (<2 kV) were obtained showing homogeneous distributions of copper and nickel oxides on the surface of the catalysts. For the catalysts C-3 and C-4, the copper and nickel aluminates which were formed, respectively, by calcination at the highest temperature (1173 K), are more highly dispersed on the γ-alumina surface (particle sizes <6 nm). Nonporous formations of the copper spinel $CuAl_2O_4$ phases, were also observed by SEM for catalyst C-5 [37,38,40–42].

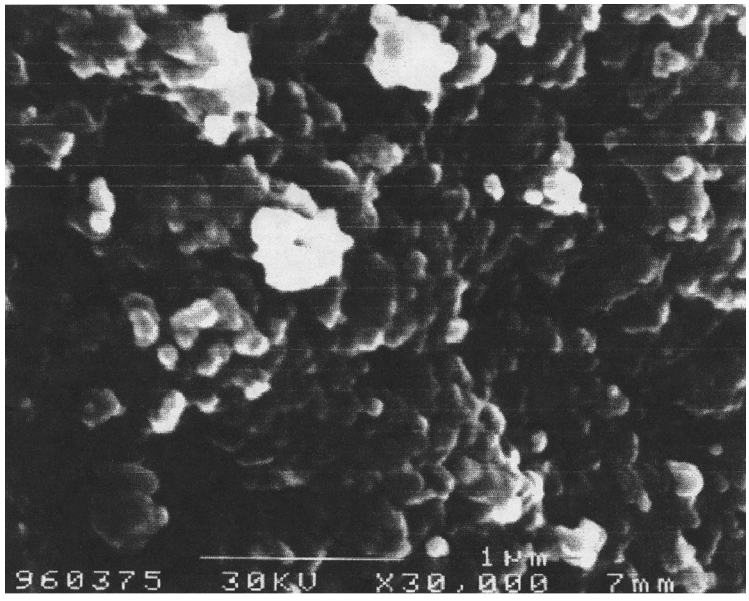

Fig. 2. Scanning electron micrograph of the C-1 sample.

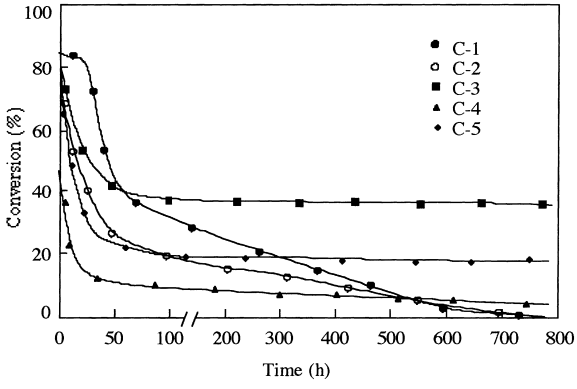

Fig. 3. Evolution of the phenol conversion for the catalysts C-1 to C-5.

3.4. Catalytic activities

Fig. 3 shows the conversions during a 33-day run for the catalytic oxidation of phenol in aqueous solutions using catalysts C-1 to C-5, under the experimental conditions given in the experimental section. The phenol conversion depends on the time of operation and type of catalyst. As can be seen, catalyst C-1 has three activity zones. In zone 1, at the beginning of the reaction (first 20 h), the catalyst C-1 shows an approximate constant phenol conversion of 80%. We may reasonably expect free copper oxide to be mainly responsible for the initial higher catalytic activity in this first plateau [37]. Next, in zone 2, phenol conversion rapidly decreases from 80 to ≈40% in ca. 2 days. After that, phenol conversion decreases more slowly and steadily to zero conversion (zone 3). Catalyst C-2 shows similar trends of phenol conversions as a function of time (see Fig. 3). There are now only two zones. A rapid decrease of phenol conversion is observed in zone 1 which takes place during the first 48 h of reaction. This effect is followed by a steady conversion decrease in zone 2 which results in the deactivation of the catalyst. The decrease in the conversion for the nickel catalyst is lower, ca. 1/2, than for the copper ones. It seems that the nickel oxide is more stable under the acidic conditions produced during the reaction process or that its reaction mechanism is different. It should also be pointed out that the nickel catalysts (C-2 and C-4) always have lower phenol conversions than the copper catalysts (C-1 and C-3), respectively.

Furthermore, catalysts C-3, C-4 and C-5 (after an induction time of 100 h) show a steady region of phenol conversion vs. time with conversion in the 40, 10 and 20% range, respectively. It can be seen

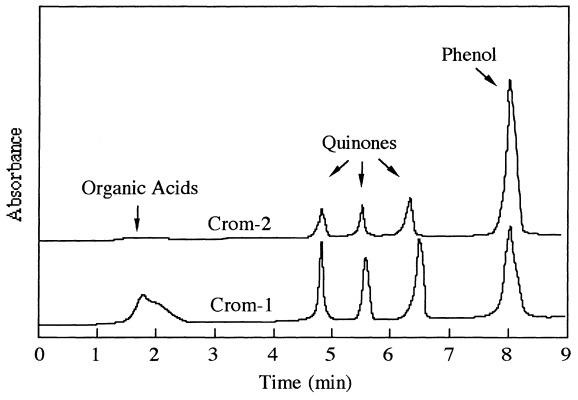

Fig. 4. Typical products detected by HPLC from copper C-1, C-3 and C-5 (Crom-1) and nickel C-2 and C-4 (Crom-2) catalysts.

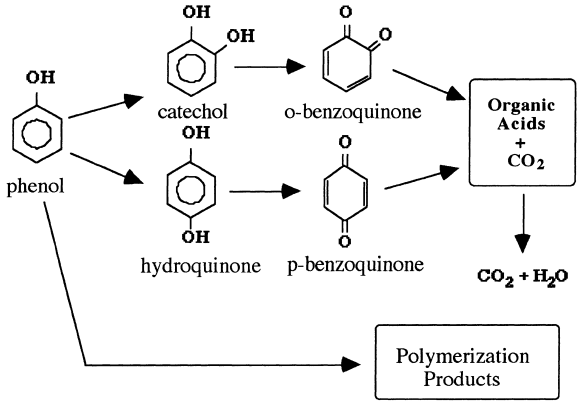

Fig. 5. Simplified reaction pathway of the phenol oxidation reaction.

that the copper and nickel aluminates are stable at the reaction conditions tested and, that, the copper aluminate catalysts are always more active than the nickel aluminate ones. The two copper aluminate catalysts C-3 and C-5 obtained by different procedures (see above), show different specific rates for phenol conversion and this effect is due to the BET area values of the catalysts.

The reaction products obtained were monitored by HPLC, and Fig. 4 shows the product distributions for the catalysts tested, which may be classified into three large categories, i.e. CO_2, carboxylic acids (mainly oxalic, acetic and succinic acids in concentration ratios of 10/5/1, respectively) and quinones–diphenols [37]. The mechanism of the oxidation of phenols is extremely complex and is not yet fully understood. It is generally accepted that the oxidation of phenol by molecular oxygen is basically an electrophillic reaction and the rate limiting step is the reaction between the aryloxy radical with oxygen [16,29]. At elevated temperatures, and in the presence of water and catalyst, oxygen is capable of different oxidation reactions, i.e. it can substitute an oxygen atom into an aromatic ring to form a dihydric phenol or quinone; oxygen is also capable of attacking carbon double bonds to form carbonyl compounds, and in oxidising alcohols and carbonyl groups to form carboxylic acids [7]. Furthermore, the greater part of the reaction products for all the catalysts are CO_2 (mainly), oxalic acid, *p*-benzoquinone, formic acid, acetic acid, succinic acid and catechol, that is in agreement with the simplified pathway for the phenol oxidation reaction showed in Fig. 5 [32].

On the other hand, the formation of polymers during the phenol oxidation reaction has also been reported [32]. These polymers can be formed by two reactions in the liquid phase caused by the addition of glyoxal to phenol or the polymerisation of glyoxal. This homogeneous polymerisation reaction markedly reduces the extent of total phenol oxidation. It is important to mention that, in the reaction conditions of this study, no formation of polymerisation products has been detected [37], which is in contrast to the data in the literature using other reactors [30,32] but in agreement with runs conducted in a differentially operated fixed-bed reactor [43]. This may be because of the high solid-to-liquid phase ratio characteristic of a trickle-bed regime, which prevents the formation of polymers. Thus, the oxidation rate measured is only the result of the heterogeneously catalysed reaction.

So, using a trickle-bed reactor, the activity loss in catalysts C-1 and C-2 cannot be explained by the formation of polymers, which might cause a poisoning effect on the catalytic sites. This activity loss, however, can easily be explained by the disappearance of CuO, NiO and copper oxalate dissolved because of the hot acidic medium due to the reaction conditions.

Fig. 6 shows the Cu and Ni concentration profiles in the reaction products during the reaction process for catalyst C-1 and C-2 due to the loss of copper and nickel, carried out by the effect of the hot acidic aqueous solution produced during the reaction. It

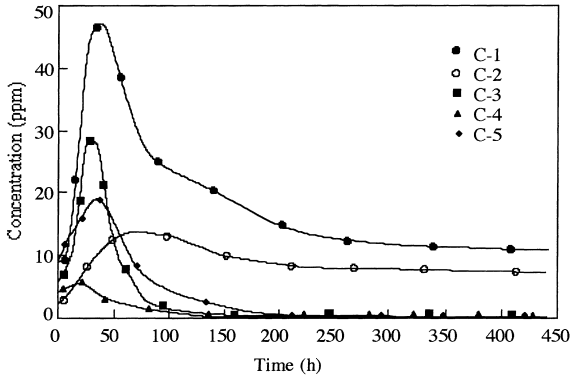

Fig. 6. Cu and Ni concentration profiles during the reaction process for the catalysts C-1 to C-5.

confirms the disappearance of Cu and Ni, as do the XRD results. During the first 100-h run, all the catalysts show a significant loss of copper and nickel ions. However, after the first 100-h run, the nickel and copper aluminate catalysts (C-3, C-4 and C-5) show a loss of concentration which is always lower than 1 ppm of copper and nickel.

Another important feature which can be extracted from the HPLC figure is the significant decrease in intermediate oxidation products, namely quinones and carboxylic acids obtained from nickel catalysts C-2 and C-4 which mainly convert phenol into CO_2 (>95%) (see Fig. 4). In contrast, the copper catalysts have a CO_2 conversion of ca. 80%. It seems that nickel catalysts are less efficient at cleaving the phenol ring (which is the limiting step of the oxidation process) but surprisingly are more active at transforming the quinones and carboxylic acids to CO_2 than the copper catalysts. Hence, although nickel catalysts have lower specific rates than copper catalysts, they seem to contain mainly specific surface-active sites for the complete oxidation of phenol to CO_2. This is of interest because it may significantly affect the life of the catalyst.

4. Conclusions

Five catalysts based on CuO/γ-alumina (C-1), NiO/γ-alumina (C-2), $CuAl_2O_4$ (C-3 and C-5) and $NiAl_2O_4$ (C-4) have been structurally characterised by BET, porosimetry, X-ray diffraction (XRD) and scanning electron microscopy (SEM). Their catalytic behaviours have also been tested for the oxidation of 5 g/l phenol aqueous solutions using a trickle-bed triphasic tubular reactor and air with an oxygen partial pressure of 0.9 MPa at a temperature of 413 K.

Here, C-1 to C-4 have surface areas of the same order as the supported γ-alumina of ca. 190 m^2/g, whereas C-5 has a surface area of ca. 30 m^2/g. C-1 to C-4 showed high active-phase dispersions which were also confirmed by SEM.

XRD detects the phases present and shows a continuous loss of eluted CuO and NiO and the formation of a copper oxalate phase in C-1 and C-3 which also elutes with time. The copper and nickel aluminate active phases are stable throughout the reaction.

The plot of phenol conversion vs. time shows that, for C-1 and C-2, there is an overall decrease in activity with several slopes reaching conversion values close to zero after a continuous working run of 1000 h. In turn, C-2, C-4 and C-5 reach steady activity plateaus at phenol conversions of 40, 10 and 20%, respectively, within 48 h of starting deactivation. HPLC monitoring of the reaction products show that copper catalysts C-1, C-3 and C-5 drive a mechanism of partial phenol oxidation to carboxylic acids and quinone-related products with very high specific rates. In turn, nickel catalysts C-2 and C-4 mainly drive a mechanism of CO_2 formation with lower conversion but with a potential higher catalyst life. It has also been found that the trickle-bed triphasic tubular reactor largely avoided the mechanism of polymer formation as a catalyst deactivation process.

References

[1] K. Lanouette, Chem. Engn., Oct. (1977) 99.
[2] E. Creary, Ohio River Valley Water Sanitation Commission Report. Cincinnati, OH, June 15, 1951.
[3] C. Comninellis, Process Safety Environ. Protect. 70(4) (1992) 219–224.
[4] H. Fenton, J. Chem. Soc. 65 (1894) 899.
[5] Y. Yamamoto, E. Niki, H. Shiokawa, J. Org. Chem. 44 (1979) 2137.
[6] M.D. Gurol, Ozone in phenolic aqueous solution: Decomposition and reaction with aqueous solutions of phenols, Ph.D. Dissertation, University of North Carolina. Chapel HiII, 1980.
[7] H. Devlin, I. Harris, Ind. Eng. Chem. Fundam. 23 (1984) 387.

[8] E. Plattner, C. Comninellis, in: S. Stucki (Ed.), Process Technology for Water Treatment, Plenum, New York, 1988, p. 205.
[9] L. Ukrinczykl, M.B. Mcbride, Clay and Clay Minerals 70(2) (1992) 157–166.
[10] D. Kirk, S. Shafirian, F. Foulkes, J. Appl. Electrochem. 15 (1985) 285.
[11] C. Comninellis, Trans IChem E. 70 (part B) (1992) 219.
[12] C. Comninellis, A. Nerini, J. Appl. Electrochem. 25(1) (1995) 23–28.
[13] A. Boudenne, O. Cerclier, J. Galea, E. Vandenllist, Appl. Cata. A-General 143(2) (1996) 185–202.
[14] T. Randall, P. Knopp, J. Water Pollut. Control. Fed. 52 (1980) 2117.
[15] J. Foussard, H. Debellefontaine, J. Environ. Eng. 115 (1989) 367.
[16] H. Joglekar, S. Samant, J. Joshi, Water Res. 25 (1991) 135.
[17] K. Fajerweg, H. Debellefontaine, Appl. Catal. B. Environmental 10(4) (1996) 229–235.
[18] K. Fajerweg, J.N. Foussard, A. Perrard, H. Debellefontaine, Water Science Techn. 35(4) (1997) 103–110.
[19] L. Palmisano, M. Schiavello, A. Sclafani, G. Martra, Appl. Catal. B: Environmental 3(2–3) (1994) 117–132.
[20] S.A. Walker, P.A. Christensen, K.E. Shaw, G.M. Walker, J. Electroanal. Chem. 393(1–2) (1995) 137–140.
[21] H. Yang, C. Eckert, Ind. Eng. Chem. Res. 27 (1988) 2009.
[22] T. Thornton, P. Savage, J. Supercritical Fluids 3 (1992) 321.
[23] S. Gopalan, P.E. Savage, AICHE J. 41(8) (1995) 1864–1873.
[24] Zy. Ding, Snuch Aki, M.A. Abraham, Envir. Sci. Tech. 29(11) (1995) 2748–2753.
[25] M. Krajnc, J. Levec, AICHE J. 42(7) (1996) 1977–1984.
[26] M. Krajncm, J. Levec, Appl. Catal. B: Environmental 3(2–3) (1994) 101–107.
[27] M. Koo, W.K. Lee, C.H. Lee, Chem. Eng. Sci. 52(7) (1997) 1201–1214.
[28] H. Tagaya, Y. Suzuki, J. Kadokawa, M. Karasu, Chem. Lett. N1 (1997) 47–48.
[29] A. Sadana, J. Katzer, J. Catal. 35 (1974) 140.
[30] H. Ohta, S. Goto, Ind. Eng. Chem. Fundam. 19 (1980) 180.
[31] R. Willms, A. Balinski, D. Harrison, Ind. Eng. Chem. 19 (1980) 180.
[32] A. Pintar, J. Levec, J. Catal. 135 (1992) 345.
[33] A. Pintar, J. Levec, J. Chem. Eng. Sci. 47 (1992) 2395.
[34] A. Fortuny, C. Ferrer, C. Bengoa, J. Font, A. Fabregat, Catal. Today 24 (1995) 79.
[35] A. Pintar, J. Levec, Catal. Today 24 (1995) 51–58.
[36] A. Pintar, J. Levec, Ind. Eng. Chem. Res. 33(12) (1994) 3070–3077.
[37] A. Alejandre, F. Medina, A. Fortuny, P. Salagre, J.E. Sueiras, Appl. Cat. B: Environmental 16 (1998) 53–67.
[38] A. Alejandre, F. Medina, A. Fabregat, P. Salagre, J.E. Sueiras. 3rd World Congress of Oxidation Catalysis, San Diego, USA, 1997.
[39] J.F. Le Page, Applied Heterogeneous Catalysis, Editions Technip, Paris 1987, pp. 42–44.
[40] M. Lo Jacono, A. Cimino, M. Inversi, J. Catal. 76 (1982) 320.
[41] D. Susnitzky, C. Carter, J. Mater. Res. 6 (1991) 1958.
[42] S. Ciampi, V. Di Castro, Surf. Interf. Anal. 22 (1994) 594.
[43] A. Pintar, J. Levec, Studies in Surface Science and Catalysis 110: 3rd World Congress on Oxidation Catalysis, 1997, p. 633.
[44] J. Zielinsky, J. Catal. 76 (1982) 157.
[45] P. Salagre, J.L.G. Fierro, F. Medina, J.E. Sueiras, J. Mol. Catal. 106 (1996) 125.